Journal of Power Sources 208 (2012) 242–247

Contents lists available at SciVerse ScienceDirect

Journal of Power Sources

journal homepage: www.elsevier.com/locate/jpowsour

Short communication

Investigation of nanostructured platinum–nickel supported on the titanium surface as electrocatalysts for alkaline fuel cells

L. Tamašauskaitė-Tamašiūnaitė[a,*], A. Balčiūnaitė[a,b], A. Vaiciukevičienė[a,c], A. Selskis[a], V. Pakštas[a]

[a] State Research Institute, Center for Physical Sciences and Technology, Institute of Chemistry, A. Goštauto 9, LT-01108 Vilnius, Lithuania
[b] Faculty of Chemistry, Vilnius University, Naugarduko 24, LT-03225 Vilnius, Lithuania
[c] Vilnius Pedagogical University, Studentų 39, LT-08106 Vilnius, Lithuania

ARTICLE INFO

Article history:
Received 10 November 2011
Received in revised form 24 January 2012
Accepted 10 February 2012
Available online 3 March 2012

Keywords:
Platinum–nickel
Titanium
Borohydride
Methanol
Ethanol
Oxidation

ABSTRACT

This study involves the formation of nanostructured platinum–nickel supported on the titanium surface catalysts using the galvanic displacement technique and investigation of their electrocatalytic activity toward the oxidation of borohydride, methanol and ethanol in an alkaline media by cyclic voltammetry and chronoamperometry. Scanning electron microscopy, Energy Dispersive X-ray Spectroscopy and X-ray diffraction were used to characterize the surface structure, composition and morphology. The nanoPt(Ni)/Ti and nanoPt/Ti catalysts exhibited a higher catalytic efficiency to the oxidation of borohydride, ethanol and methanol as compared with that of pure Pt.

1. Introduction

Direct alcohol fuel cells (DAFCs) are being developed especially for portable power supply. Since borohydride, methanol and ethanol are used as fuel, the development of electrocatalysts having a high electroactivity for their oxidations is of considerable interest to fuel cells. It is well known that platinum is an effective electrocatalyst for oxidation of borohydride [1–13], methanol and ethanol [14–26]. Unfortunately, the use of platinum as an electrode material is limited by its scarcity and price. Alloying Pt with transition metals such as Ni, Co and Fe allows reducing its cost and provides better catalytic characteristics for oxidation of borohydride [4,8,13], methanol [24,26,27] or reduction of oxygen [28–33]. Bimetallic catalysts usually are of better activity and stability than the monometallic ones. The catalytic enhancement of Pt alloys with transition metals has been attributed to the PtM alloy formation and the Pt electronic structure change due to the presence of M, Pt–Pt distance, and d-electron density in Pt [12,27–41].

Recently, the titanium surface has been used as a support for the fabrication of catalysts. The electrochemical activity of titanium-supported PtSn/Ti, Pt_3Ti electrodes was investigated toward the oxidation of formic acid and methanol [42–44]. Electrooxidation of methanol was also studied on the titanium mesh coated with a $PtRuO_x$ catalyst [45], the platinized Ti electrode [46] and on Pt finely dispersed on Ti metal [47]. The catalytic activity of carbon-supported PtTi alloy for molecular oxygen electroreduction was evaluated in [48]. In all cases these catalysts show an enhanced catalytic activity.

In the present study we present a simple approach to fabricate the nano-scale bimetallic platinum–nickel catalyst supported on the titanium surface (denoted as nanoPt(Ni)/Ti) via the galvanic displacement technique [13,41,49–53]. The electroless nickel was used as an underlayer for producing the Pt particles on the titanium surface. The electrocatalytic activity of the as-prepared nanoPt(Ni)/Ti catalyst and the one electrochemically treated in sulfuric acid (denoted as nanoPt/Ti) catalysts was examined in respect to the oxidation of borohydride, methanol and ethanol in an alkaline media by cyclic voltammetry (CV) and chronoamperometry (CA). The surface morphology, composition and structure of the samples were characterized using Scanning Electron Microscopy (SEM), Energy Dispersive X-ray Spectroscopy (EDAX) and X-ray diffraction (XRD).

2. Experimental details

2.1. Chemicals

Titanium foil (99.7% purity of 0.127 mm thickness), $NaBH_4$ and H_2PtCl_6 were purchased from Sigma–Aldrich Supply. H_2SO_4 (96%), NaOH (98.8%), ethanol and methanol were purchased from

* Corresponding author. Tel.: +370 5 266129; fax: +370 5 2649774.
E-mail address: lortam@ktl.mii.lt (L. Tamašauskaitė-Tamašiūnaitė).

0378-7753/$ – see front matter © 2012 Elsevier B.V. All rights reserved.
doi:10.1016/j.jpowsour.2012.02.079

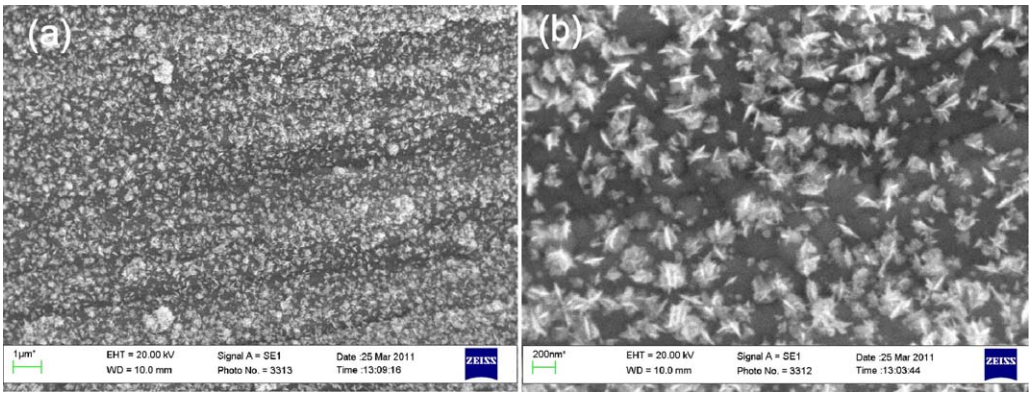

Fig. 1. SEM micrographs of as-prepared nanoPt(Ni)/Ti under different magnifications.

Chempur Company. All chemicals were of analytical grade. Deionized water was used to prepare all the solutions.

2.2. Fabrication of catalysts

The Pt–Ni catalyst was deposited on the titanium surface using the galvanic displacement technique. At first, a thin layer of Ni was deposited on the titanium surface. Briefly, prior to electroless Ni deposition, titanium sheets (1 cm × 1 cm) were degreased with ethanol, rinsed with deionized water and dried in an Ar stream. Then, the titanium surface was activated in a 0.5 g l^{-1} $PdCl_2$ solution for 1 min, followed by rinsing of the treated surface with deionized water and then immersed into the electroless nickel solution containing 0.1 M nickel sulfate, 0.4 M glycine, 0.25 M sodium hyphophosphite and 0.1 M disodium malonate at a constant temperature of 85 °C for 1 min. The solution pH was maintained at 9.0. Then the Ni/Ti electrodes were immersed in the solution containing 1 mM H_2PtCl_6 and 0.1 M HCl at room temperature for 15 min. The surface-to-volume ratio was 1.3 dm^2 l^{-1}. After plating, the samples were taken out, thoroughly rinsed with deionized water and dried in air at room temperature. Then, the fabricated catalysts were used for electro-oxidation of borohydride, methanol and ethanol without any further treatment.

2.3. Characterization of catalysts

The structure and morphology of the nanoPt(Ni)/Ti and nanoPt/Ni catalysts were characterized by Scanning Electron Microscope with Energy Dispersive and Wave Dispersion X-ray Spectrometers (Oxford, UK). Pt metal loading was estimated using STRATAGEM software and EDS K-ratios for Ni, P, Ti and O K alpha lines and Pt L alpha lines.

XRD patterns were measured using an X-ray diffractometer D8 Advance (Bruker AXS, Germany) with Cu K_α radiation. The grazing incidence method ($\omega = 0.5°$) with step-scan mode was used in the 2Θ range from 10° to 80° with a step size of 0.04° and a counting time of 6 s per step.

2.4. Electrochemical measurements

A conventional three-electrode electrochemical cell was used for cyclic voltammetry. The nanoPt(Ni)/Ti, nanoPt/Ti and Ni/Ti electrodes were employed as the working electrodes, an $Ag/AgCl/KCl_{sat}$ electrode was used as a reference electrode and a Pt sheet was used as a counter electrode. The borohydride oxidation was tested in a 1.0 M NaOH solution containing 0.05 M $NaBH_4$. The ethanol and methanol oxidations were tested in a 0.5 M NaOH solution containing 2.0 M CH_3OH and C_2H_5OH, respectively. The electrolyte solutions were prepared using p.a. grade chemicals and deionized water. All electrochemical measurements were performed with a Metrohm Autolab potentiostat (PGSTAT100) using Electrochemical Software (Nova 1.6.013). Steady state linear sweep voltammograms were recorded at a linear potential sweep rate of 50 mV s^{-1} from the stationary E_S value in the anodic direction up to 0.6 V in the alkaline borohydride solution and 0.3 V in the alkaline methanol and ethanol solutions at 25 °C.

The platinum electroactive surface area (ESA) in the catalyst was estimated from the charge associated with the formation and stripping of the adsorbed H monolayer (210 μC cm^{-2}) [54].

The chronoamperometric measurements were carried out by, at first, holding the potential at open circuit for 10 s, then stepping to potentials −0.8 and 0.3 V for 130 s in the borohydride alkaline solution and to −0.25 V for 130 s in the methanol and ethanol solutions, respectively.

3. Results and discussion

The nanoPt(Ni)/Ti catalysts were fabricated using a simple and low-cost electroless deposition method followed by galvanic displacement of Ni. The thin electroless nickel film of about 300 nm was chosen as an underlayer for the formation of immersion platinum overlayer onto the titanium surface. Due to galvanic displacement platinum deposition, nonspherical platinum crystallites were formed on the Ni surface. The morphology of the as-prepared nanoPt(Ni)/Ti structure was studied using SEM. The SEM images of the catalyst at different magnifications presented in Fig. 1a and b reveal the presence of nano-scale dendrites with the sizes of ca. 50–100 nm. Light oblong sticks can be resolved in these dendrites.

The presence of Pt and Ni onto the titanium surface was confirmed further by Energy Dispersive X-ray analysis. According to the data of EDAX analysis, the nanoPt(Ni)/Ti composition was: Pt – 1.49 at.%, Ni – 24.60 at.%, P – 6.81 at.%, O – 25.73 at.% and Ti – 41.37 at.%. It is seen, that a significant quantity of deposited nickel and a much lower amount of Pt on the electrode surface were detected. Noteworthy the nickel layer is deposited on the titanium surface from the electroless plating solution using hyphophosphite as a reducing agent. The presence of this reductor results in the deposition of Ni layer containing about 7 at.% of P.

It has been determined that the Pt loading was 18.1 μg Pt cm^{-2} in the as-prepared nanoPt(Ni)/Ti catalyst after sonication of the Ni/Ti surface in a platinum-containing solution for 15 min.

Typical cyclic voltammograms of nanoPt/Ti (*solid line*) and pure Pt (*dotted line*) electrodes in 0.5 M H_2SO_4 are shown in Fig. 2. The CV profile of the nanoPt(Ni)/Ti catalyst shows the usual characteristics of Pt since Ni is electrochemically leached, furthermore, the current for hydrogen adsorption/desorption and oxide formation/reduction on the nanoPt(Ni)/Ti catalyst is much higher than

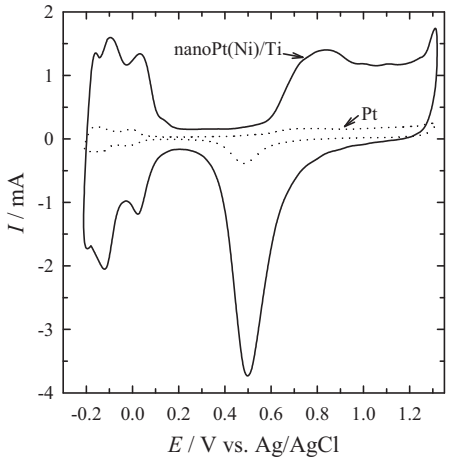

Fig. 2. CVs of pure Pt (*dotted line*) and nanoPt(Ni)/Ti (*solid line*) in 0.5 M H_2SO_4 at a sweep rate of 50 mV s^{-1}.

that on Pt. As the Ni particles are not fully covered with Pt and during the electrochemical treatment Ni is leached, so the remaining deposits are fully protected by Pt. The hydrogen adsorption charge (Q_H) of polycrystalline Pt was calculated at 0.315 mC cm^{-2}. The nanoPt(Ni)/Ti produced Q_H of 1.41 mC cm^{-2}. The calculated electroactive surface area (ESA) values are 2.85 and 12.8 cm^2 for pure Pt and nanoPt(Ni)/Ti, respectively. The roughness factors are 1.4 and 6.4 for Pt and nanoPt(Ni)/Ti, respectively. These results show that the ESA of the sample is about 4.5 times higher than that of polycrystalline Pt. According to the data of EDAX analysis the composition of the latter catalyst was as follows: Pt – 0.47 at.%, Ni – 10.67 at.%, P – 1.18 at.%, O – 29.42 at.% and Ti – 58.26 at.%. Smaller amounts of Ni and Pt were detected on the Pt/Ti surface. The data confirm that a portion of Ni which was not covered with Pt leached out from the surface during the catalyst treatment in sulfuric acid. A slightly smaller Pt loading of 16.5 μg Pt cm^{-2} was determined in this catalyst as compared with that of the as-prepared nanoPt(Ni)/Ti catalyst.

The XRD pattern presented in Fig. 3 was measured for the as-prepared nanoPt(Ni)/Ti. Sharp peaks marked with a sign of filled square are attributable to a titanium substrate (PDF no. 44-1294). Vertical dashed lines with a sign of filled circle on the top indicate positions of XRD peaks of nickel according to PDF no. 4-850. Dashed lines with empty circles show positions of Pt diffraction peaks (PDF no. 4-802). Lines marked with upside-down triangle indicate positions of maxima of the experimental XRD peaks measured at 2Θ angles of 46.5° and ~66°. The maximums are slightly

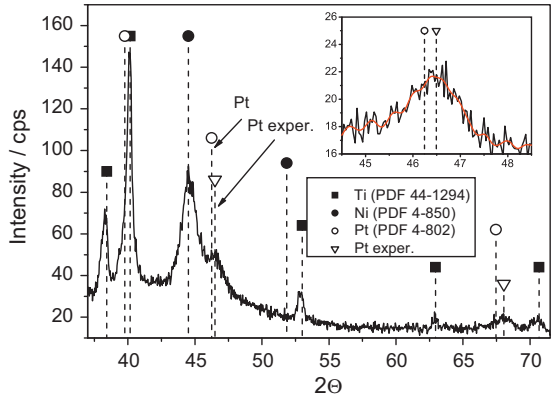

Fig. 3. XRD pattern for the nanoPt(Ni)/Ti. The inset shows the XRD peak at 2Θ angle of 46.5°.

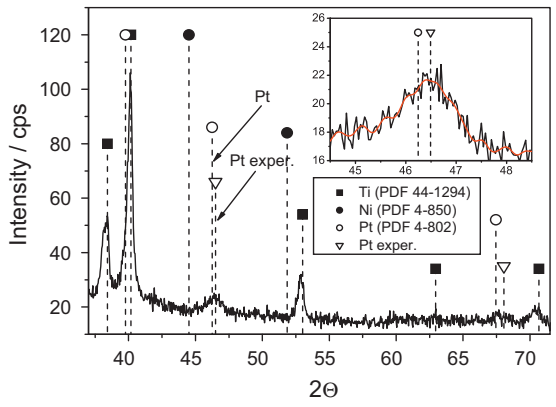

Fig. 4. XRD pattern for the Pt/Ti. The inset shows the XRD peak at 2Θ angle of 46.5°.

shifted toward higher 2Θ angles with respect to Pt peak position (the inset in Fig. 3). This means that the XRD peaks at 2Θ angles of 46.5° and ~66° are attributable to a substitution solid solution of nickel in platinum. Fig. 4 represents XRD pattern for the latter catalyst after its treatment in 0.5 M H_2SO_4 at 50 mV s^{-1}. It is evident that pure Ni fully dissolved since XRD peak at ~44.4° disappeared while peaks at 2Θ angles of 46.5° and ~66° are still seen. This means that the solid solution of Ni in platinum remained after the dissolution of nickel.

The electrochemical activity of the nanoPt(Ni)/Ti and nanoPt/Ti catalysts toward the oxidation of borohydride, ethanol and methanol was evaluated in an alkaline media using cyclic voltammetry and chronoamperometry. Fig. 5 presents stabilized cyclic voltammograms (CVs) of pure Pt (*dotted line*), Ni/Ti (*dashed line*), nanoPt/Ti (*dash-dot line*) and nanoPt(Ni)/Ti (*solid line*) in 1.0 M NaOH containing 0.05 M $NaBH_4$ at 50 mV s^{-1}. In the forward sweep toward positive potential values two well-distinguished anodic peaks: peak I at lower potential values and peak II at more positive potential values are seen in the CVs plots for the pure Pt, as-prepared nanoPt(Ni)/Ti and the latter catalyst treated electrochemically in 0.5 M H_2SO_4 at 50 mV s^{-1}. The shape of cyclic voltammograms for the as-prepared nanoPt(Ni)/Ti and nanoPt/Ti catalysts is similar to the CV onto pure Pt (Fig. 5), furthermore, the oxidations peaks are significantly higher in the case nanoPt(Ni)/Ti than those on pure Pt or nanoPt/Ti catalysts. As described in literature the anodic oxidation of borohydrides is postulated as follows:

$$BH_4^- + 8OH^- \rightarrow BO_2^- + 6H_2O + 8e^- \quad (1)$$

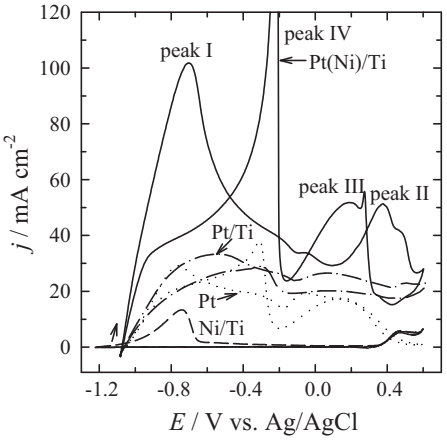

Fig. 5. CVs of pure Pt (*dotted line*), nanoNi/Ti (*dashed line*), nanoPt(Ni)/Ti (*solid line*) and nanoPt/Ti (*dash-dot line*) in a 1.0 M NaOH solution containing 0.05 M $NaBH_4$ at 50 mV s^{-1}.

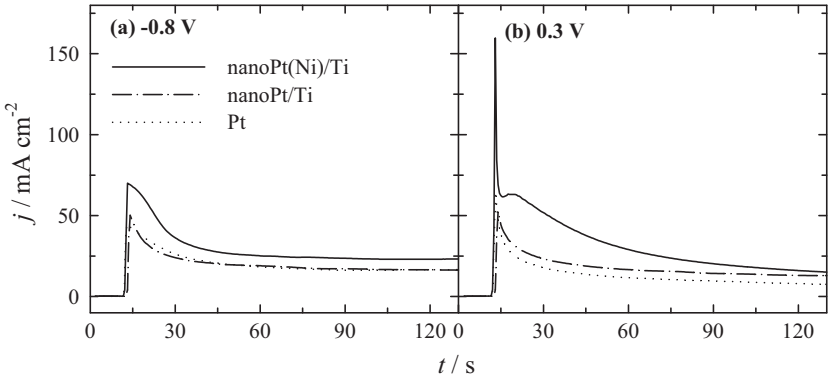

Fig. 6. Chronoamperometric data from nanoPt(Ni)/Ti (*solid lines*), nanoPt/Ti (*dash-dot line*) and Pt (*dotted lines*) catalysts studied at −0.8 (a) and 0.3 V (b) in a 1.0 M NaOH containing 0.05 M $NaBH_4$ solution. The potential was firstly held at open circuit for 10 s, then set to −0.8 and 0.3 V, respectively.

It has been determined that both on nickel and Pt [1,2,55–63] the quasi-spontaneous hydrolysis during which a hydroxyl borohydride intermediate and hydrogen are generated by various steps (Eqs. (2) and (3)) occurs in competition with the borohydride oxidation reaction (Eq. (1)):

$$BH_4^- + H_2O \rightarrow BH_3OH^- + H_2 \quad (2)$$

$$BH_3OH^- + H_2 \rightarrow BO_2^- + 3H_2 \quad (3)$$

and the overall reaction of BH_4^- ion oxidation on these metals proceeds through a four-electron process (Eq. (4)):

$$BH_4^- + 4OH^- \rightarrow BO_2^- + 2H_2O + 2H_2 + 4e^- \quad (4)$$

Anodic peak I seen in CVs for Pt, Ni/Ti, nanoPt/Ti and nanoPt(Ni)/Ti catalysts (Fig. 5) is attributed to the oxidation of H_2 generated by catalytic hydrolysis of BH_4^- as described in [56–58] (borohydride oxidation releases molecular hydrogen on nickel). The current density of peak I for the nanostructured electrode is about 3 times higher than that on pure Pt or nanoPt/Ti. Peak II which is attributed to direct borohydride oxidation [1,9] is also about 2–3 times higher as compared to that of pure Pt or nanoPt/Ti, but it is shifted to positive potential values by 0.3 V. Reverse peaks III and IV appear at about the same potential values for the investigated catalysts, while the nanoPt(Ni)/Ti catalyst produces higher current densities. However, assuming ca. 4.5-fold higher active surface area of Pt(Ni)/Ti compared to smooth polycrystalline Pt, the surface area normalized borohydride oxidation current is ca. 1.5-times higher on Pt. This could be due to ability to oxidize evolved hydrogen at Pt sites, whereas the Pt dendrites are not fully covering the substrate (see Fig. 1b).

In the case of the Ni/Ti electrode (Fig. 1, *dashed line*), anodic peak I at a lower potential values of about −0.8 V is observed in the CV. During the subsequent anodic scans no anodic peaks were observed on this catalyst in the potential region from −1.0 to 0.3 V (Fig. 1, *dashed line*). It may be suggested that the Ni–P layer deposited on the titanium surface does not catalyze the direct borohydride oxidation at higher potentials due to the passivation caused by nickel (hydr)oxide(s) formation [64,65] or, maybe, the surface of catalyst is poisoned by strongly adsorbed intermediates generated during the oxidation of borohydride [1]. Since the Ni/Ti catalyst shows no electroactivity toward the direct electrooxidation of borohydride, an enhanced electrocatalytic activity of the as-prepared nanoPt(Ni)/Ti catalyst may be ascribed to PtNi alloy formation and Pt electronic structure change due to the presence of Ni [12,30]. Although the PtNi alloy formation was also observed in the nanoPt/Ti catalyst according to the XRD data (Fig. 3), the lower anodic currents were measured at this catalyst. It may be due to the collapsing of Pt particles which is caused by the Ni (not covered with Pt) anodic dissolution during the electrochemical treatment of the as-prepared nanoPt(Ni)/Ti catalyst in sulfuric acid [39].

The performance of nanoPt(Ni)/Ti, nanoPt/Ti and Pt catalyst for the oxidation of H_2 generated by catalytic hydrolysis of BH_4^- (peak I) and borohydride oxidation (peak II), can be further observed from chronoamperometric measurements. The corresponding curves are shown in Fig. 6. The investigated catalysts show a current decay for both reactions. At the end of experimental period (t = 130 s), the current density of the nanoPt(Ni)/Ti is higher and the current density decay is much slower than that on Pt or nanoPt/Ti. The nanoPt(Ni)/Ti catalyst has a higher catalytic activity and a better stability for hydrogen and borohydride oxidation as compared to those of Pt or nanoPt/Ti. Therefore, the nanoPt/Ti catalyst shows higher oxidation currents than those of pure Pt (Fig. 6b). This result is in agreement with the results of cyclic voltammetry curves. Active surface area normalized currents are about 2–3-fold higher at Pt for both oxidations of hydrogen and borohydride than those on nanoPt(Ni)/Ti under chronoamperometric conditions.

Fig. 7 presents stabilized cyclic voltammograms after a long-term potential cycling (after 10 cycles) for Ni/Ti, nanoPt(Ni)/Ti, nanoPt/Ti and pure Pt in a 0.5 M NaOH containing 2.0 M C_2H_5OH (a) and 2.0 M CH_3OH (b) at 50 mV s^{-1}. As seen from Fig. 7, the voltammetric curves for oxidation of ethanol (a) and methanol (b) on the nanoPt(Ni)/Ti and nanoPt/Ti catalysts are similar in shape to those obtained on the bulk Pt, except for enhanced currents. During the anodic scans, the nanoPt(Ni)/Ti electrocatalyst shows a higher ethanol oxidation currents and at lower potential values (peak I) as compared with those at nanoPt/Ti (Fig. 7a), indicating that nanoPt/Ti is less active for ethanol oxidation than the as-prepared nanoPt(Ni)/Ti electrocatalyst. However, 2–3 times enhanced current densities for ethanol oxidation are obtained on the both catalysts as compared with those on pure Pt (Fig. 7a). Active surface area normalized currents are about 1.5–2-fold lower on the nanoPt(Ni)/Ti and nanoPt/Ti catalysts as compared to those on Pt in ethanol solution.

The nanoPt/Ti catalyst exhibits a higher electrocatalytic activity toward the oxidation of methanol as compared to that of the as-prepared nanoPt(Ni)/Ti. Therefore, about 37 and 45 times higher current densities for methanol oxidation are obtained on the nanoPt(Ni)/Ti and nanoPt/Ti electrodes, respectively, as compared with that on pure Pt. The active surface area normalized currents for methanol oxidation is about 8–10-fold higher on nanoPt(Ni)/Ti and nanoPt/Ti, respectively, than that on pure Pt. Inasmuch, the Ni/Ti electrode shows no electrocatalytic activity toward the oxidation of ethanol and methanol (Fig. 7, *dashed lines*), the observed enhanced anodic currents at the nanoPt/Ti and nanoPt(Ni)/Ti catalysts under the potential region −0.8 and 0.3 V are also attributed to a strong change in Pt electronic properties caused by the Ni [35,37,39–41].

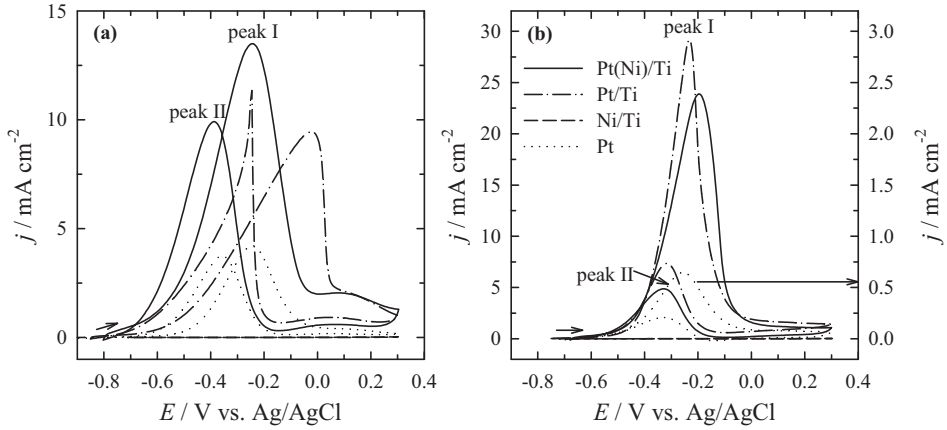

Fig. 7. CVs of pure Pt (*dotted lines*), nanoNi/Ti (*dashed line*), nanoPt/Ti (*dash-dot line*) and nanoPt(Ni)/Ti (solid lines) in a 0.5 M NaOH solution containing 2.0 M C_2H_5OH (a) and 2.0 M CH_3OH (b) at 50 mV s^{-1}.

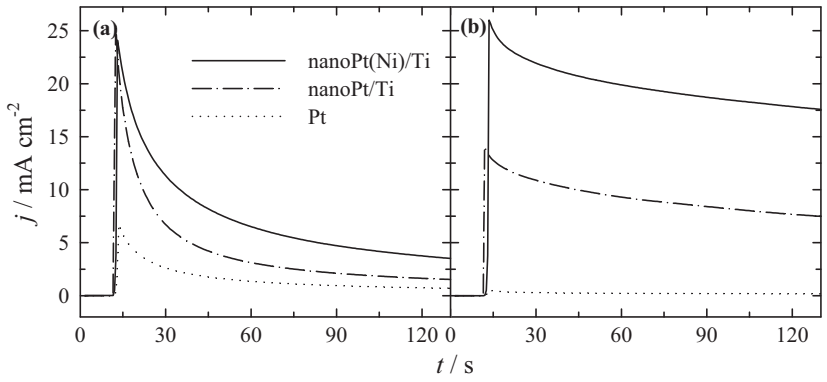

Fig. 8. Chronoamperometric data from Pt (*dotted line*), nanoPt/Ti (*dash-dot line*) and nanoPt(Ni)/Ti (*solid lines*) catalysts studied at −0.25 V in a 0.5 M NaOH containing 2.0 M C_2H_5OH (a) and 2.0 M CH_3OH (b). The potential was firstly held at open circuit for 10 s, then set to −0.25 V.

A high electroactivity of nanoPt(Ni)/Ti and nanoPt/Ti catalysts compared to that of Pt was also tested by the chronoamperometry method in alkaline solutions of ethanol (a) and methanol (b). Fig. 8 shows the chronoamperometric data at −0.25 V for the investigated catalysts. The current density for ethanol oxidation on the nanoPt(Ni)/Ti and nanoPt/Ti catalysts is much higher and current density decay is much slower as compared to that on pure Pt (Fig. 8a). A significant increase in steady-state current density for methanol oxidation on the both catalysts occurs in comparison to pure Pt (Fig. 8b). The steady-state current densities of nanoPt(Ni)/Ti, nanoPt/Ti and pure Pt are 17.57, 7.47 and 0.17 mA cm^{-2} (t = 130 s), respectively. This shows that the oxidation rate of methanol at −0.25 V on nanoPt(Ni)/Ti and nanoPt/Ti is about 100 and 43 times, respectively, higher than that on Pt. Active surface area normalized currents are about of 0.7 mA cm^{-2} for ethanol oxidation on nanoPt(Ni)/Ti and 0.5 mA cm^{-2} on the nanoPt/Ti and Pt catalysts, therefore, the active surface area normalized currents for methanol oxidation are about 22-fold and 9.5-fold higher on nanoPt(Ni)/Ti and nanoPt/Ti, respectively, than those on pure Pt.

The as-prepared nanoPt(Ni)/Ti catalyst and the latter catalyst electrochemically treated in sulfuric acid show better performance for oxidation of both ethanol and methanol as compared to that on pure Pt. A higher current density is obtained on these catalysts for methanol oxidation as compared to that for ethanol oxidation.

4. Conclusions

In this study we have successfully fabricated an electrode modified with platinum crystallites on the titanium surface, as a substrate, using a simple and low-cost method. For the displacement deposition of Pt crystallites on the titanium surface, the Ni adlayer was used as a precursor. It has been determined that the average size of the Pt crystallites deposited by galvanic displacement of Ni adlayer is about 50–100 nm. The as-prepared nanoPt(Ni)/Ti catalyst with the Pt loading of 18.1 μg Pt cm^{-2} and the latter catalyst treated electrochemically in sulfuric acid with the Pt loading of 16.5 μg Pt cm^{-2} were found to be more active than Pt toward the electro-oxidation of borohydride, methanol and ethanol in the alkaline media. Also, the nanoPt(Ni)/Ti catalyst shows better voltammetric and chronoamperometric performance for methanol oxidation than for ethanol oxidation.

The fabricated nanoPt(Ni)/Ti catalysts seem to be a promising anodic material for direct alkaline fuel cells. Further investigation is underway.

Acknowledgments

This research was funded by the grant (No. ATE-03/2010) from the Research Council of Lithuania. The authors express their gratitude to Habil. Dr. Z. Jusys from the Institute of Surface Chemistry and Catalysis, Ulm University for helpful discussions.

References

[1] E.L. Gyenge, Electrochim. Acta 49 (2004) 965–978.
[2] B.H. Liu, Z.P. Li, S. Suda, Electrochim. Acta 49 (2004) 3097–3105.
[3] J.H. Kim, H.S. Kim, Y.M. Kang, M.S. Song, S. Rajendran, S.C. Han, D.H. Jung, J.Y. Lee, J. Electrochem. Soc. 151 (2004) A1039–A1043.

[4] E.L. Gyenge, M.H. Atwan, D.O. Northwood, J. Electrochem. Soc. 153 (2006) A150–A158.
[5] K. Deshmukh, K.S.V. Santhanam, J. Power Sources 159 (2006) 1084–1088.
[6] A. Verma, S. Basu, J. Power Sources 174 (2007) 180–185.
[7] J.I. Martins, M.C. Nunes, R. Koch, L. Martins, M. Bazzaoui, Electrochim. Acta 52 (2007) 6443–6449.
[8] X. Geng, H. Zhang, W. Ye, Y. Ma, H. Zhong, J. Power Sources 185 (2008) 627–632.
[9] J.I. Martins, M.C. Nunes, J. Power Sources 175 (2008) 244–249.
[10] B.M. Concha, M. Chatenet, Electrochim. Acta 54 (2009) 6119–6129.
[11] G. Rostamikia, M.J. Janik, Electrochim. Acta 55 (2010) 1175–1183.
[12] G.J. Wang, Y.Z. Gao, Z.B. Wang, C.Y. Du, J.J. Wang, G.P. Yin, J. Power Sources 195 (2010) 185–189.
[13] A. Tegou, S. Papadimitriou, I. Mintsouli, S. Armyanov, E. Valova, G. Kokkinidis, S. Sotiropoulos, Catal. Today 170 (2011) 126–133.
[14] C. Lamy, J.M. Leger, J. Clavier, J. Electroanal. Chem. 135 (1982) 321–328.
[15] B. Beden, F. Kadirgan, C. Lamy, J.M. Leger, J. Electroanal. Chem. 142 (1982) 171–190.
[16] E. Morallon, J.L. Vazquez, A. Aldaz, J. Electroanal. Chem. 288 (1990) 217–228.
[17] A.V. Tripkovic, K.Dj. Popovic, J.D. Momcilovic, D.M. Drazic, J. Electroanal. Chem. 418 (1996) 9–20.
[18] F. Goaguen, J.-M. Leger, C. Lamy, J. Appl. Electrochem. 27 (1997) 1052–1060.
[19] A.V. Tripkovic, K.Dj. Popovic, J.D. Momcilovic, D.M. Drazic, J. Electroanal. Chem. 448 (1998) 173–181.
[20] E.H. Yu, K. Scott, R.W. Reeve, J. Electroanal. Chem. 547 (2003) 17–24.
[21] Y. Ishikawa, M.-Sh. Liao, C.R. Cabrera, Surf. Sci. 463 (2000) 66–80.
[22] M. Umeda, M. Kokubo, M. Mohamedi, I. Uchida, Electrochim. Acta 48 (2003) 1367–1374.
[23] G.A. Camara, T. Iwasita, J. Electroanal. Chem. 578 (2005) 315–321.
[24] L. Colmenares, E. Guerrini, Z. Jusys, K.S. Nagabhushana, E. Dinjus, S. Behrens, W. Habicht, H. Bonnemann, R.J. Behm, J. Appl. Electrochem. 37 (2007) 1413–1427.
[25] M.J. Giz, G.A. Camara, J. Electroanal. Chem. 625 (2009) 117–122.
[26] X. Wang, Ch. Hu, Y. Xiong, H. Liu, G. Du, X. He, J. Power Sources 196 (2011) 1904–1908.
[27] E. Antolini, J.R.C. Salgado, A.M. Dos Santos, E.R. Gonzalez, Electrochem. Solid State Lett. 8 (2005) A226–A230.
[28] E. Antolini, J.R.C. Salgado, E.R. Gonzalez, Appl. Catal. B: Environ. 63 (2006) 137–149.
[29] S. Mukerjee, S. Srinivasan, M.P. Soriaga, J. McBreen, J. Electrochem. Soc. 142 (1995) 1409–1415.
[30] T. Toda, H. Igarashi, H. Uccida, M. Watanabe, J. Electrochem. Soc. 146 (1999) 3750–3759.
[31] T. Toda, H. Igarashi, M. Watanabe, J. Electroanal. Chem. 460 (1999) 258–262.
[32] V. Stamenkovic, T.J. Schmidt, P.N. Ross, N.M. Markovic, J. Phys. Chem. B 106 (2002) 11970–11979.
[33] L. Xiong, A. Manthiram, J. Mater. Chem. 14 (2004) 1454–1460.
[34] H.A. Gasteiger, S.S. Kocha, B. Sompalli, F.T. Wagner, Appl. Catal. B: Environ. 56 (2005) 9–35.
[35] A. Ruban, B. Hammer, P. Stoltze, H.L. Skriver, J.K. Nørskov, J. Mol. Catal. A: Chem. 115 (1997) 421–429.
[36] M.M. Jaksic, Int. J. Hydrogen Energy 26 (2001) 559–578.
[37] J.R. Kitchin, N.A. Khan, M.A. Barteau, J.G. Chen, B. Yakshinskiy, T.E. Madey, Surf. Sci. 544 (2003) 295–308.
[38] J.R. Kitchin, J.K. Nørskov, M.A. Barteau, J.G. Chen, J. Chem. Phys. 120 (2004) 10240–10246.
[39] J. Greeley, M. Mavrikakis, Nat. Mater. 3 (2004) 810–815.
[40] J. Greeley, M. Mavrikakis, Catal. Today 111 (2006) 52–58.
[41] S. Papadimitriou, A. Tegou, E. Pavlidou, S. Armyanov, E. Valova, G. Kokkinidis, S. Sotiropoulos, Electrochim. Acta 53 (2008) 6559–6567.
[42] Q. Yi, J. Zhang, A. Chen, X. Liu, G. Xu, Z. Zhou, J. Appl. Electrochem. 38 (2008) 695–701.
[43] H.B. Hassan, J. Fuel Chem. Technol. 37 (2009) 346–354.
[44] H. Abe, F. Matsumoto, L.R. Alden, S.C. Warren, H.D. Abruña, F.J. DiSalvo, J. Am. Chem. Soc. 130 (2008) 5452–5458.
[45] E.H. Yu, K. Scott, Electrochem. Commun. 6 (2004) 361–365.
[46] Z.-G. Shao, W.-F. Lin, F. Zhu, P.A. Christensen, H. Zhang, B. Yi, J. Power Sources (2006) 1003–1008.
[47] R.G. Freitas, M.C. Santos, R.T.S. Oliveira, L.O.S. Bulhões, E.C. Pereira, J. Power Sources 158 (2006) 164–168.
[48] E. Ding, K.L. More, T. He, J. Power Sources 175 (2008) 794–799.
[49] S.R. Brankovic, J. McBreen, R.R. Adzic, J. Electroanal. Chem. 503 (2001) 99–104.
[50] K. Sasakia, J.X. Wang, H. Naohara, N. Marinkovic, K. More, H. Inada, R.R. Adzic, Electrochim. Acta 55 (2010) 2645–2652.
[51] D. Gokcen, S.-E. Bae, S.R. Brankovic, J. Electrochem. Soc. 157 (2010) D582–D587.
[52] D. Gokcen, S.-E. Bae, S.R. Brankovic, Electrochim. Acta 56 (2011) 5545–5553.
[53] A. Tegou, S. Armyanov, E. Valova, O. Steenhaut, A. Hubin, G. Kokkinidis, S. Sotiropoulos, J. Electroanal. Chem. 634 (2009) 104–110.
[54] H. Angerstein-Kozlowska, B.E. Conway, W.B.A. Sharp, J. Electroanal. Chem. 43 (1973) 9–36.
[55] M.E. Indig, R.N. Snyder, J. Electrochem. Soc. 109 (1962) 1104–1106.
[56] B.H. Liu, Z.P. Li, S. Suda, J. Electrochem. Soc. 150 (2003) A398–A402.
[57] K.M. Gorbunova, M.V. Ivanov, V.P. Moiseev, J. Electrochem. Soc. 120 (1973) 613–618.
[58] J.S. Walter, A. Zurawski, D. Montgomery, M. Thornburg, S. Revankar, J. Power Sources 179 (2008) 335–339.
[59] R. Jasinski, Electrochem. Technol. 3 (1965) 40.
[60] U.B. Demirci, J. Power Sources 172 (2007) 676–687.
[61] J. Ma, N.A. Choundry, Y. Sahai, Renew. Sust. Energy Rev. 14 (2010) 183–199.
[62] J.H. Morris, H.J. Gysing, D. Reed, Chem. Rev. 85 (1985) 51–76.
[63] J.A. Gardiner, J.W. Collat, J. Am. Chem. Soc. 87 (1965) 1692–1700.
[64] Ch. Zhang, S.M. Park, J. Electrochem. Soc. 134 (1987) 2966–2970.
[65] M. Wehrens-Dijksma, P.H.L. Notten, Electrochim. Acta 51 (2006) 3609–3621.